Large scale dissipation and filament instability in two-dimensional turbulence

Large Scale Dissipation and Filament Instability in Two-Dimensional Turbulence

Dalila Elhmaidi
Laboratoire de Mécanique des Fluides, Faculté des Sciences de Tunis, Tunisia

Jost von Hardenberg and Antonello Provenzale
ISAC–CNR, Torino and CIMA, Savona, Italy
(Received 24 December 2004; published 1 July 2005)

Coherent vortices in two-dimensional turbulence induce far-field effects that stabilize vorticity filaments and inhibit the generation of new vortices. We show that the large-scale energy sink often included in numerical simulations of statistically stationary two-dimensional turbulence reduces the stabilizing role of the vortices, leading to filament instability and to continuous formation of new coherent vortices. This counterintuitive effect sheds new light on the mechanisms responsible for vortex formation in forced-dissipated two-dimensional turbulence, and it has significant impact on the temporal evolution of the vortex population in freely decaying turbulence. The time dependence of vortex statistics in the presence of a large-scale energy sink can be approximately described by a modified version of the scaling theory developed for small-scale dissipation.

DOI: 10.1103/PhysRevLett.95.014503 PACS numbers: 47.27.Eq, 47.20.Ft, 47.32.Cc

Two-dimensional (2D) barotropic turbulence is one of the simplest theoretical models used to describe the dynamics of rotation-dominated turbulent geophysical flows in the ocean and the atmosphere [1,2]. Barotropic turbulence is characterized by the presence of strong coherent vortices that live for a large number of vortex rotation periods [3–6]. The vortices account for a large portion of the energy and the enstrophy (squared vorticity) of the flow [5,6], trap fluid for long times [7,8], and induce non-Gaussian velocity distributions in the surrounding turbulent flow, with significant effects on particle transport [9–12].

The dynamics of 2D (or barotropic) turbulence on the horizontal plane (x, y) and as a function of time t is described by the vorticity equation

$$\frac{D\omega}{Dt} \equiv \frac{\partial \omega}{\partial t} + J(\psi, \omega) = D_{\mathrm{high}} + D_{\mathrm{low}} + F, \qquad (1)$$

where $\omega = \nabla^2\psi$ is vorticity, $\psi(x, y, t)$ is the stream function, and ∇^2 is the horizontal Laplacian. The symbol $J(\psi, \omega)$ denotes the Jacobian, $J(a, b) = \frac{\partial a}{\partial x}\frac{\partial b}{\partial y} - \frac{\partial b}{\partial x}\frac{\partial a}{\partial y}$. The symbols D_{high} and D_{low} denote dissipation operators at high and low wave numbers, respectively, and F indicates a forcing term. At large Reynolds number (i.e., when dissipation and forcing are small enough), a random initial vorticity field evolves spontaneously into an ensemble of coherent vortices [3,5,13]. The coherent vortices are immersed in a background turbulent field that contains a large number of vorticity filaments, generated during dissipative interactions such as vortex merging and vortex stripping.

When dissipation is present but forcing is absent, the turbulent flow is freely decaying, and the system tends, on long times, to a state of rest. Usually, freely decaying turbulence is dissipated only at small scales, with a dissipation operator of the form $D_{\mathrm{high}} = (-1)^{n-1}\nu_n\nabla^{2n}\omega$, where ν_n is a viscosity coefficient and n defines the order of the viscosity operator [3,6,13]. For $n = 1$, standard Newtonian viscosity is recovered, and $n > 1$ corresponds to hyperviscosity. Note that, in general, hyperviscosity is taken as a parametrization of the small-scale energy sink associated with unresolved processes.

In order to obtain a statistically stationary flow in the presence of dissipation, forcing must be introduced. Because of the inverse cascade, in forced turbulence energy piles up at the scales of the simulation domain and a large-scale energy sink becomes necessary [5,7,14,15]. Large-scale dissipation is typically obtained by a hypoviscosity term, $D_{\mathrm{low}} = (-1)^{m-1}K_m\nabla^{-2m}\omega$, where m is a positive constant. This form confines dissipation at very low wave numbers. In the following, we use the value $m = 1$, which gives $D_{\mathrm{low}} = K_1\psi$. Physically, large-scale dissipation is taken as a parametrization of the large-scale energy sinks associated with the presence of Rossby waves (due to topography and/or variations in the Coriolis parameter), free-surface effects, interaction with the bottom and the boundaries, and interaction with stable circulation systems at large scales. In this work we show that the presence of a large-scale energy sink significantly affects filament dynamics.

When no vortices are present, isolated vorticity filaments are unstable and roll up to form new vortices [16]. In freely decaying turbulence with small-scale dissipation, filaments generated during vortex interactions are stabilized by the presence of the vortices and do not roll up [16–20]. In such conditions, barotropic vortices exert their stabilizing influence to large distances, due to the logarithmic form of the Green's function for 2D flows [10,11]. Modifications of the Green's function that reduce the range of the interactions, such as the presence of strong baroclinicity, reduce the stabilizing effect of the vortices [21,22].

In statistically stationary, forced-dissipated 2D turbulence, the number of vortices remains approximately constant in time; new coherent vortices are necessarily generated as the vortices have a finite lifetime. Some mechanism that overcomes the stabilizing effect of the vortices must thus be present. One such mechanism is the forcing itself, which allows vorticity peaks in the background to grow into coherent vortices [23]. As discussed here, another mechanism is associated with the presence of the large-scale energy sink, which breaks the far-field effect of the vortices and allows for filament instability, even in the absence of forcing.

To illustrate this effect, we first consider the case of an individual merging event. We numerically integrate the vorticity Eq. (1) with a pseudospectral code on a doubly periodic domain $(2\pi, 2\pi)$ with a spatial resolution of 256^2 collocation points [7,20]. We include small-scale dissipation and no forcing, and we consider two cases characterized by the presence or absence of a large-scale energy sink. Here we use hyperviscosity with $n = 4$ and, when present, hypoviscosity with $m = 1$. The initial condition is given by a pair of same-sign identical vortices with the Gaussian profile, $\omega(r) = \omega_0 \exp(-\frac{r^2}{r_0^2})$ with $r_0 = \pi/5$. The initial distance between the two vortex centers is $d = 2\pi/5$, which is less than the critical merging distance for these vortices [24].

Figure 1 shows the outcome of the merging when only small-scale dissipation is present (left panel) and when large-scale dissipation is also active (right panel). During vortex merging, vorticity filaments are ejected, and they form an almost circular ring around the merged vortices. When only small-scale dissipation is present, no filament instability is detected, as the filaments are stabilized by the long-range strain field induced by the central vortices [16–18,20]: Filaments are stable when the square ratio of filament vorticity to the strain field induced by the vortices, $\Lambda^2 = \omega_f^2/S_v^2$, is less than $\Lambda_0^2 = 0.25$ [here, $S_v^2 = (\partial_x u - \partial_y v)^2 + (\partial_x v + \partial_y u)^2$]. When large-scale dissipation is included, the situation changes dramatically. The presence of a large-scale energy sink reduces the long-range inhibiting effect of the vortices, and the filaments can undergo instability and roll-up.

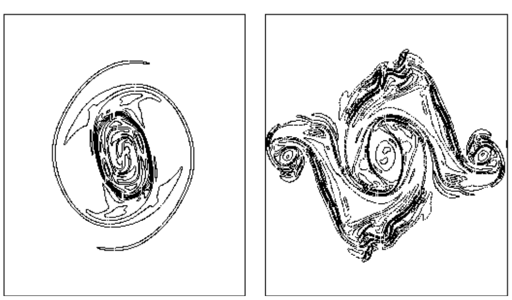

FIG. 1. Vorticity contours after the merging of two same-sign vortices when only small-scale dissipation is present (left) and also when a large-scale energy sink is present (right). The initial conditions are the same for the two cases.

Filament vorticity has its main spectral components at small scale, while the far field of the vortices is dominated by the long-wave components. These components are most readily eliminated by large-scale dissipation, which damps more effectively the long-range velocity field induced by the vortices than the small-scale filament vorticity. Figure 2 shows the energy spectra after the merging, $E(k)$, both with (dashed line) and without (solid line) large-scale dissipation. As expected, without a large-scale energy sink the spectrum is peaked at the scale of the simulation box, $k = 1$, and the behavior of the velocity field has a strong nonlocal component. With large-scale dissipation, nonlocality is broken, the energy content at large scales decreases with time, and the energy spectrum peaks at an intermediate wave number. The inset of Fig. 2 shows the temporal evolution of the parameter Λ^2 (averaged over the area outside the central vortices) for the two cases with and without large-scale dissipation. When only small-scale dissipation is present, Λ^2 stays below 0.25, and the filaments are stable. When large-scale dissipation is also present, Λ^2 is above 0.25, and the filaments are unstable.

The presence of filament instability has major effects on the evolution of the vortex population that emerges from random initial conditions. To illustrate this, we numerically integrate the unforced 2D vorticity Eq. (1) on a square periodic domain $(2\pi, 2\pi)$ with resolution 1024^2 grid points. For consistency with previous works [6,13], we use small-scale dissipation with $n = 2$ and $\nu_2 = 2.2 \times 10^{-10}$. Large-scale dissipation, when present, has order $m = 1$ and $K_1 = 1$ [25]. The initial vorticity field has a narrow-band energy

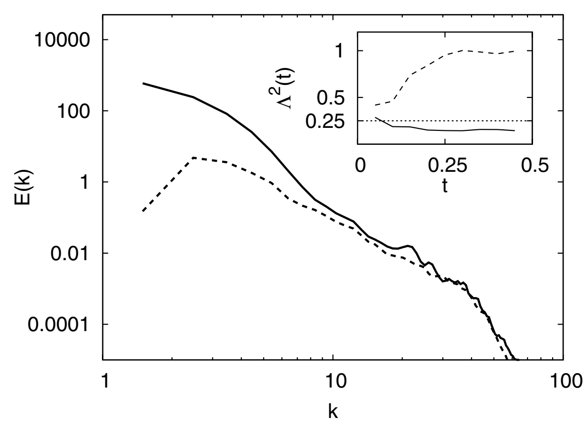

FIG. 2. Energy spectrum after merging, as a function of the radial wave number, k. The solid line is for the case where no large-scale dissipation is present, and the dashed line refers to the case with a large-scale energy sink. The inset shows the time evolution of the stability parameter $\Lambda^2 = \omega_f^2/S_v^2$ without (solid line) and with (dashed line) large-scale dissipation. The line at $\Lambda_0^2 = 0.25$ separates stable filaments for $\Lambda^2 < \Lambda_0^2$ from unstable filaments for $\Lambda^2 > \Lambda_0^2$ [20].

spectrum $E(k) \propto k^6/(1 + k/k_0)^{18}$ with $k_0 = 60$ and total energy $E_k = \int E(k)dk = 0.5$ [13].

Figure 3 shows the time evolution of the number of vortices when only small-scale dissipation is present (solid curve) and when large-scale dissipation is also added (dashed line). The vortices have been identified by the vortex census algorithm described in [11–13]. In the absence of large-scale dissipation, the number of vortices decays according to the scaling theory of Carnevale *et al.* with a scaling exponent $\xi = 0.72$ [26,27].

The addition of a large-scale energy sink slows down the decay of the number of vortices: Some of the filaments produced during vortex merging become unstable, and, as a result, the decay in the total number of vortices is slower. At time $T = 20$, one observes approximately 30% more vortices when large-scale dissipation is present. However, kinetic energy decreases faster when large-scale dissipation is present: At time $T = 20$ the kinetic energy of the flow with no large-scale dissipation is $E_k(T) = 0.97E_k(0)$, while that of the flow that is dissipated also at large scales is $E_k(T) = 0.38E_k(0)$. Naively, one could have expected that a faster decay of kinetic energy would have led to a faster decrease of the vortex number. This is not the case, because of the mechanism of filament instability that is triggered by the large-scale energy sink.

Experimentation with the intensity of the large-scale dissipation, K_1, shows a dependence of the effect on the value of K_1. When K_1 is too large, the vortex population is rapidly dissipated. When K_1 is too small, the far-field stabilizing effect of the existing vortices is not eliminated and few new vortices are generated. In order to see filament instability and generation of new vortices, the large-scale dissipation should be in an intermediate range where it can affect the far field of the vortices without destroying them.

Since the new vortices are generated by filament instability, one expects an excess of small vortices in comparison to the case with small-scale dissipation only. Figure 4 shows the time evolution of the average vortex radius for the two cases. When large-scale dissipation is present, the average vortex radius is smaller, and it grows more slowly than predicted by the scaling theory. The inset of Fig. 4 shows the histogram of the vortex radii, $n(r)$, at time $t = 15$: A much larger number of small vortices is present when large-scale dissipation is active, while the number of vortices with larger radius is approximately unchanged.

The results reported above indicate that when a large-scale energy sink is present, the scaling theory discussed by Carnevale *et al.* [26,27] does not immediately describe the evolution of the vortex population. In fact, large-scale dissipation leads to a significant decay of kinetic energy, contrary to what is observed in the case of small-scale dissipation only. However, both the kinetic energy carried by the vortices, $E_{k,v} = N\zeta_a^2 r_a^4$, where ζ_a is the average peak vorticity of the vortices and r_a is the average vortex radius, and the average peak vorticity itself remain approximately constant. This indicates that most of the energy dissipation takes place in the background and suggests that a scaling theory may still approximately hold. In addition, at late times the vortex number decays approximately as a power law, $N(t) \propto t^{-\beta}$ with $\beta \approx 0.52$. Using this value for the scaling exponent, we obtain estimates for the growth rate of the average vortex radius and for the average vortex circulation [27]. Figure 5 shows the vortex number N, the average vortex radius r_a, and the average vortex circulation Γ_a as a function of time, together with the predictions of the scaling theory with $\beta = 0.52$. At late times, a good agreement between the numerical results and the modified scaling theory is observed.

An interesting question concerns the difference between the value of the scaling exponent with and without large-

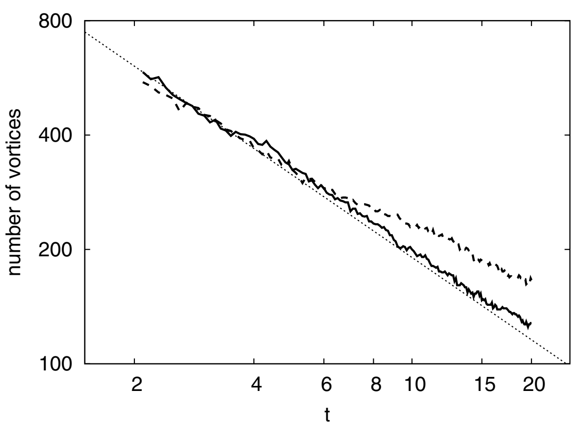

FIG. 3. Number of vortices as a function of time, starting from random initial conditions, when only a small-scale dissipation is present (solid line) and when a large-scale energy sink is also included (dashed line). The dotted line shows the prediction of the scaling theory of Carnevale *et al.* [26,27].

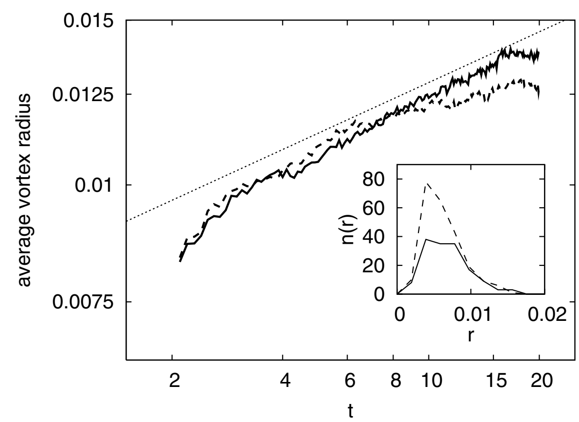

FIG. 4. Average vortex radius as a function of time, starting from random initial conditions, when only small-scale dissipation is present (solid line) and when a large-scale energy sink is also included (dashed line). The dotted line shows the prediction of the scaling theory of Carnevale *et al.* [26]. The inset shows the histogram of the vortex radii at time $t = 15$ without (solid line) and with (dashed line) the large-scale energy sink.

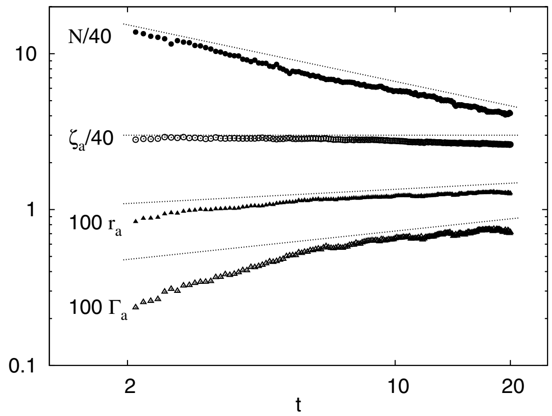

FIG. 5. Time evolution of the vortex number, N (solid circles), of the average vortex radius, r_a (solid triangles), of the average peak vorticity, ζ_a (empty circles), and of the average vortex circulation, Γ_a (empty triangles), when both small and large-scale dissipation are present. The dotted lines indicate the predictions of the scaling theory with modified scaling exponent $\beta = 0.52$, obtained from a fit to the decay of the vortex number.

scale dissipation. The scaling theory of Carnevale *et al.* has been rationalized in terms of the outcome of vortex merging events, by making the hypothesis that the merging of two vortices always leads to only one vortex. When large-scale dissipation is present, filaments produced by the merging can become unstable and roll up into one or more small new vortices. In this case, the outcome is not always just one vortex. This suggests an extension of the approach based on ''punctuated Hamiltonian dynamics'' [27,28], where the outcome of point vortex merging is allowed to be, with some low probability, more than one vortex.

The results discussed in this Letter indicate that the direct action of the forcing is not the only mechanism that can generate new vortices from background vorticity peaks. Another mechanism, which has been discussed here, is filament instability and subsequent roll-up, favored by the presence of a large-scale energy sink that breaks the far-field effect of the vortices. It is intriguing, and counterintuitive, that adding dissipation allows the vortex population to survive for a longer time. Other processes may have a similar effect, such as the presence of a stably stratified temperature field coupled with two-dimensional turbulence [29], or the presence of magnetic effects. It would be interesting to verify whether proper modifications of the scaling theory of Carnevale *et al.* apply also to these cases. In fact, any process that breaks the long-range inhibitory effect of the coherent vortices may allow for the birth of new vortices and for a renewal of the vortex population.

[1] R. Kraichnan and D. Montgomery, Rep. Prog. Phys. **43**, 547 (1980).
[2] R. Salmon, *Lectures on Geophysical Fluid Dynamics* (Oxford University Press, Oxford, 1998).
[3] J. C. McWilliams, J. Fluid Mech. **146**, 21 (1984).
[4] R. Benzi, G. Paladin, S. Patarnello, P. Santangelo, and A. Vulpiani, J. Phys. A **19**, 3771 (1986).
[5] A. Babiano, C. Basdevant, B. Legras, and R. Sadourny, J. Fluid Mech. **183**, 379 (1987).
[6] J. C. McWilliams, J. Fluid Mech. **219**, 361 (1990).
[7] D. Elhmaïdi, A. Provenzale, and A. Babiano, J. Fluid Mech. **257**, 533 (1993).
[8] A. Provenzale, Annu. Rev. Fluid Mech. **31**, 55 (1999).
[9] A. Bracco, J. Lacasce, and A. Provenzale, J. Phys. Oceanogr. **30**, 461 (2000).
[10] A. Bracco, J. Lacasce, C. Pasquero, and A. Provenzale, Phys. Fluids **12**, 2478 (2000).
[11] C. Pasquero, A. Provenzale, and A. Babiano, J. Fluid Mech. **439**, 279 (2001).
[12] C. Pasquero, A. Provenzale, and J. Weiss, Phys. Rev. Lett. **89**, 284501 (2002).
[13] A. Bracco, J. McWilliams, G. Murante, A. Provenzale, and J. Weiss, Phys. Fluids **12**, 2931 (2000).
[14] V. Borue, Phys. Rev. Lett. **71**, 3967 (1993).
[15] V. Borue, Phys. Rev. Lett. **72**, 1475 (1994).
[16] N. Kevlahan and M. Farge, J. Fluid Mech. **346**, 49 (1997).
[17] D. Dritschel, J. Fluid Mech. **206**, 193 (1989).
[18] D. Dritschel, P. Haynes, M. Juckes, and T. Sheperd, J. Fluid Mech. **230**, 647 (1991).
[19] N. Balmforth, D. del Castillo-Negrete, and W. Young, J. Fluid Mech. **333**, 197 (1997).
[20] D. Elhmaïdi, A. Provenzale, T. Lili, and A. Babiano, Phys. Lett. A **333**, 85 (2004).
[21] J. von Hardenberg, J. McWilliams, A. Provenzale, A. Shchepetkin, and J. Weiss, J. Fluid Mech. **412**, 331 (2000).
[22] A. Bracco, J. von Hardenberg, A. Provenzale, J. Weiss, and J. McWilliams, Phys. Rev. Lett. **92**, 084501 (2004).
[23] B. Legras, P. Santangelo, and R. Benzi, Europhys. Lett. **5**, 37 (1988).
[24] M. Melander, N. Zabusky, and J. McWilliams, J. Fluid Mech. **195**, 303 (1988).
[25] If we assume large-scale dissipation to be a parametrization of the energy sink associated with Rossby wave radiation, the value $K_1 = 1$ implies that the Rhines scale, $L_\beta = (U/\beta)^{1/2}$, where β is the latitudinal gradient of the Coriolis parameter and U is a velocity scale, is equal to the box size, L. That is, $K_1 = 1$ implies that the scale above which Rossby wave dynamics is dominant coincides with the size of the simulation domain.
[26] G. Carnevale, J. McWilliams, Y. Pomeau, J. Weiss, and W. Young, Phys. Rev. Lett. **66**, 2735 (1991).
[27] J. Weiss and J. McWilliams, Phys. Fluids A **5**, 608 (1993).
[28] G. Riccardi, R. Piva, and R. Benzi, Phys. Fluids A **7**, 3091 (1995).
[29] S. Wunsch and Y.-N. Young, Phys. Rev. E **66**, 016306 (2002).